

Slow Fatigue and Highly Delayed Yielding via Shear Banding in Oscillatory Shear

James O. Cochran¹, Grace L. Callaghan¹, Miles J. G. Caven, and Suzanne M. Fielding¹
Department of Physics, Durham University, Science Laboratories, South Road, Durham DH1 3LE, United Kingdom

 (Received 21 November 2022; revised 21 November 2023; accepted 15 March 2024; published 17 April 2024)

We study theoretically the dynamical process of yielding in cyclically sheared amorphous materials, within a thermal elastoplastic model and the soft glassy rheology model. Within both models we find an initially slow accumulation, over many cycles after the inception of shear, of low levels of damage in the form strain heterogeneity across the sample. This slow fatigue then suddenly gives way to catastrophic yielding and material failure. Strong strain localization in the form of shear banding is key to the failure mechanism. We characterize in detail the dependence of the number of cycles N^* before failure on the amplitude of imposed strain, the working temperature, and the degree to which the sample is annealed prior to shear. We discuss our finding with reference to existing experiments and particle simulations, and suggest new ones to test our predictions.

DOI: [10.1103/PhysRevLett.132.168202](https://doi.org/10.1103/PhysRevLett.132.168202)

Amorphous materials [1–3] include soft solids such as emulsions, colloids, gels, and granular materials, and harder metallic and molecular glasses. Unlike crystalline solids, they lack order in the arrangement of their constituent microstructures (droplets, grains, etc.). Understanding their rheological properties is thus a major challenge. Typically, they behave elastically at low loads then yield plastically at larger loads. Much effort has been devoted to understanding the dynamics of yielding following the imposition of a shear stress σ or strain rate $\dot{\gamma}$, which is held constant after switch-on. This often involves the formation of shear bands [4], which can slowly heal away to leave homogeneous flow in complex fluids [5–15], or trigger catastrophic failure in solids [16,17]. In many applications, however, materials are subject to a *cyclically repeating* deformation or load. Cyclic shear is also important fundamentally in revealing key fingerprints of a material's nonlinear rheology, with large amplitude oscillatory shear intensely studied [18–34].

The response of an amorphous material to an oscillatory shear strain depends strongly on the strain amplitude γ_0 relative to a threshold γ_c [35–55]. For $\gamma_0 < \gamma_c$, a material typically settles into deep regions of its energy landscape, showing reversible response from cycle to cycle (after many cycles), via an absorbing state transition. The number of cycles to settle, however, diverges as $\gamma_0 \rightarrow \gamma_c^-$. For $\gamma_0 > \gamma_c$, a material instead yields into a state of higher

energy that is chaotically irreversible from cycle to cycle, and often shear banded [32,33,55–57].

Indeed, the process of repeatedly straining or loading a material over many cycles typically leads to the gradual accumulation of microstructural damage. While the early signatures of such fatigue are often difficult to detect, its slow buildup can eventually undermine material stability and precipitate catastrophic failure. Understanding the accumulation of microstructural fatigue and identifying the microscopic precursors that prefigure failure is thus central to the prediction of material stability and lifetime, and the development of strategies to improve them.

In hard materials, the buildup of microstructural damage is often interpreted in terms of the formation of microcracks. Far less well understood in soft materials, it remains the topic of intense study, as recently reviewed [58]. Colloidal gels in oscillatory stress [59–61] display an intricate, multistage yielding process in which the sample remains solidlike for many cycles, before slipping at the rheometer wall, then forming coexisting solid-fluid bulk shear bands and finally fully fluidizing [61]. The number of cycles before yielding increases dramatically at low stress amplitudes [60,61]. Particle [62] and fiber bundle [63] simulations likewise show increasing yielding delay with decreasing cyclic load amplitude. Metallic glass simulations show an increasing number of cycles to shear band formation with decreasing γ_0 [64]. Particle simulations [36,38] and experiments on colloidal glass [47] show a number of strain cycles to attain a yielded steady state diverging as $\gamma_0 \rightarrow \gamma_c^+$.

Despite this rapid experimental progress, the dynamics of yielding in cyclic shear remains poorly understood theoretically. An insightful recent study of athermal materials captured delayed yielding after a number of cycles that increases at low strain amplitude [65]. In being mean field,

Published by the American Physical Society under the terms of the [Creative Commons Attribution 4.0 International license](https://creativecommons.org/licenses/by/4.0/). Further distribution of this work must maintain attribution to the author(s) and the published article's title, journal citation, and DOI.

however, this work necessarily neglects the development of damage in the form of strain heterogeneity and shear bands that are key to understanding yielding.

In this Letter, we study theoretically the yielding of amorphous materials in oscillatory shear strain. Our contributions are fourfold. First, we predict a slow accumulation, over many cycles, of initially low levels of damage in the form of strain heterogeneity across the sample. Second, we show that this early fatigue later gives way to catastrophic material failure, after a number of cycles N^* . Third, we show that the formation of shear bands is key to the failure mechanism, as seen experimentally. Finally, we characterize the dependence of N^* on the strain amplitude γ_0 , the working temperature T , and the degree of sample annealing prior to shear.

Models.—To gain confidence that our predictions are generic across a wide range of amorphous materials, independent of specific constitutive modeling assumptions, we study numerically two different widely used models of elastoplastic rheology: the soft glassy rheology (SGR) model [66] and a thermal elastoplastic (TEP) model [1].

The SGR model comprises an ensemble of elastoplastic elements, each corresponding to a mesoscopic region of material large enough to admit a local continuum shear strain l and stress Gl , with modulus G . Under an imposed shear rate $\dot{\gamma}$, any element strains at rate $\dot{l} = \dot{\gamma}$. Elemental stresses are, however, intermittently released via local plastic yielding events, occurring stochastically at rate $r = \tau_0^{-1} \min\{1, \exp[-(E - \frac{1}{2}Gl^2)/T]\}$, with τ_0 a microscopic attempt time, E a local energy barrier, and T temperature. Upon yielding, any element resets its strain, $l \rightarrow 0$, and selects a new yield energy from a distribution $\rho(E) = \exp(-E/T_g)/T_g$. The model captures a glass transition at temperature $T = T_g$ and predicts rheological aging at low loads in its glass phase, $T < T_g$. The macroscopic elastoplastic stress σ is the average of the elemental stresses. The total stress $\Sigma = \sigma + \eta\dot{\gamma}$ includes a Newtonian contribution of viscosity η .

The TEP model is defined likewise, except each element has the same yield energy E , and after yielding selects its new l from a Gaussian of width l_h . Both models thus combine the basic ingredients of elastic deformation punctuated by plastic rearrangements and stress propagation. But whereas SGR incorporates disorder in the material's energy landscape via $\rho(E)$ to capture glassy behavior, yet neglects frustrated local stresses, the TEP model conversely neglects glassiness, but captures frustrated local stresses via the posthop l distribution.

To capture catastrophic yielding, it is crucial to allow for strain localization and shear banding. Accordingly, in each model the elastoplastic elements are arranged across S streamlines stacked in the flow gradient direction y , with M elements per streamline. The imposed shear rate, averaged across streamlines, is $\bar{\dot{\gamma}}(t)$. The local shear rate can, however, vary across streamlines: at uniform total stress

Σ in creeping flow we have $\Sigma(t) = \sigma(y, t) + \eta\dot{\gamma}(y, t) = \bar{\sigma}(t) + \eta\bar{\dot{\gamma}}(t)$, with y a streamline's flow gradient coordinate. After any local yielding event with stress drop of magnitude Δl we furthermore pick three random elements on each neighboring streamline and adjust their $l \rightarrow l + w\Delta l(-1, +2, -1)$. We thus implement 1D Eshelby stress propagation [67] and stress diffusion [68], which are key to shear banding.

Protocol.—We study oscillatory shear strain $\bar{\gamma}(t) = \gamma_0 \sin(\omega t)$, imposed for all times $t > 0$. Prior to shear, the sample is prepared via ageing or annealing. Within SGR, we perform a sudden deep quench at time $t = -t_w$ from infinite temperature to a working temperature $T < T_g$ in the glass phase, then age the sample for a waiting time t_w . Within TEP, we first equilibrate the sample to a temperature T_0 , then suddenly at time $t = 0$ quench to a working temperature $T < T_0$. Larger t_w (SGR) or smaller T_0 (TEP) corresponds to better annealing.

About an initially uniform state, tiny levels of heterogeneity are seeded naturally via M and S being finite. In SGR we also test the effect of adding a small initial perturbation to the well depths $E \rightarrow E(1 + \delta \cos 2\pi y)$. That we observe the same physics in both cases shows that our results are robust to small initial randomness.

In response to the imposed strain, we measure the shear stress $\Sigma(t)$ and report its root mean square Σ_{rms} over each cycle vs cycle number N . We also define the degree of shear banding $\Delta\dot{\gamma}(t)$ via the standard deviation of the strain rate across streamlines, normalized by $\dot{\gamma}_0 = \gamma_0\omega$, and report its mean over each cycle, $\langle \Delta\dot{\gamma} \rangle(N)$. When this quantity is high, the strain rate profile is significantly shear banded across the flow gradient direction.

Parameters.—Both models have as parameters the mean local yield energy $\langle E \rangle$, attempt time τ_0 , temperature T , number of streamlines S , elements per streamline M , Newtonian viscosity η , and stress diffusion w . The degree of annealing is prescribed by the waiting time t_w (SGR) or prequench temperature T_0 (TEP). The imposed shear has amplitude γ_0 and frequency ω . We choose units $\tau_0 = 1$, $G = 1$, $\langle E \rangle = 1$. We set $\eta = 0.05$, $w = 0.05$, $l_h = 0.05$, $\delta = 0.01$, suited to the Newtonian viscosity, stress diffusivity, and initial heterogeneity being small. We set the numerical parameters $S = 25$, $M = 10\,000$, having checked for robustness to variations in these. For computational efficiency, we set $\omega = 0.1$ in SGR, but checked that our findings also hold for $\omega = 0.01$. In TEP we set $\omega = 0.01$. We then explore yielding as a function of strain amplitude γ_0 , working temperature T , and degree of annealing before shear.

SGR results.—The key physics that we report is exemplified by Figs. 1(a) and 1(b). These show that yielding comprises two distinct stages as a function of cycle number N . In the first stage, the sample remains nearly homogeneous, with only low level material fatigue (small strain heterogeneity $\langle \Delta\dot{\gamma} \rangle$) slowly accumulating from cycle

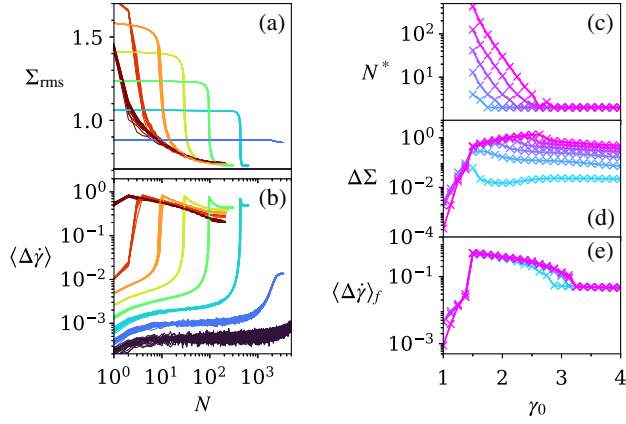


FIG. 1. SGR model. (a) Root mean square stress and (b) mean degree of shear banding over each cycle versus cycle number N for strain amplitudes $\gamma_0 = 1.00, 1.25, \dots, 2.75$ in curve sets with drops in (a) and rises in (b) right to left. Each curve within a set corresponds to a different random initial condition. $t_w = 10^7$, $T = 0.3$. (c) Cycle number at failure N^* , (d) magnitude of stress drop $\Delta \Sigma$, and (e) final degree of shear banding $\langle \dot{\gamma} \rangle_f$ vs strain amplitude γ_0 for waiting times $t_w = 10^2, 10^3, \dots, 10^7$ in curves bottom to top. Panel (c) only shows samples with $\Delta \Sigma > 0.1$. N^* , $\Delta \Sigma$, $\langle \dot{\gamma} \rangle_f$ averaged over initial condition.

to cycle, and the stress remaining high. After a delay that increases dramatically with decreasing imposed strain amplitude γ_0 in curve sets left to right, a second stage ensues: the stress drops quickly, the strain becomes highly localized into shear bands, and the sample fails catastrophically.

To quantify the delay during which fatigue slowly accumulates before the sample catastrophically fails, we define the cycle at failure N^* as that in which Σ_{rms} first falls below $\frac{1}{2}(\Sigma_{\text{max}} - \Sigma_{\text{min}})$, where Σ_{max} and Σ_{min} are the global maximum and minimum of Σ_{rms} versus N [69]. We further define the magnitude of yielding via the normalized stress drop $\Delta \Sigma = (\Sigma_{\text{max}} - \Sigma_{\text{min}})/\Sigma_{\text{SS}}$, where Σ_{SS} is the steady state stress as $N \rightarrow \infty$, and the extent to which strain becomes localized via the final degree of shear banding $\langle \Delta \dot{\gamma} \rangle_f = \lim_{N \rightarrow \infty} \langle \Delta \dot{\gamma} \rangle(N)$. These three quantities are plotted vs γ_0 in Figs. 1(c)–1(e).

Clearly apparent is a transition at strain amplitude $\gamma_0 = \gamma_c \approx 1.4$, below which the stress drop $\Delta \Sigma$ and degree of strain localization $\langle \Delta \dot{\gamma} \rangle_f$ become negligible: for $\gamma_0 < \gamma_c$, no appreciable yielding occurs. For $\gamma_0 > \gamma_c$, we see a range of γ_0 , increasing with increasing t_w , over which yielding is both strongly apparent and heavily delayed. The delay increases dramatically with decreasing γ_0 , although N^* shows no apparent divergence over the window of strains for which yielding is appreciable.

The dependence of yielding on the degree of ageing prior to shear, t_w , is further explored in Fig. 2. Panels (a) and (b) again reveal the two stage yielding just described, with curve sets left to right showing a longer delay with

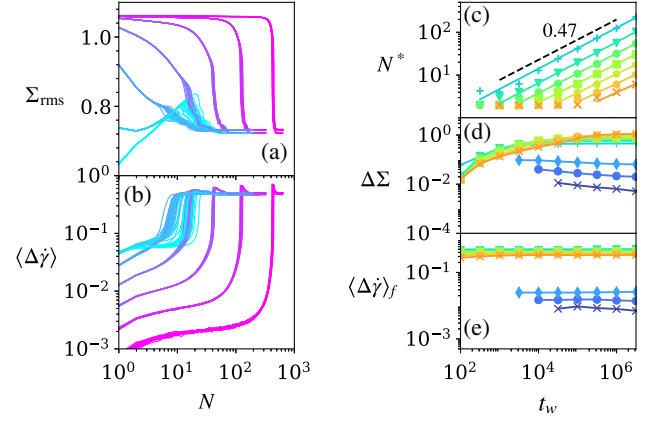


FIG. 2. SGR model. (a) Root mean square stress and (b) mean degree of shear banding over each cycle as a function of cycle number N for waiting time $t_w = 10^1, 10^2, \dots, 10^7$ in curve sets with drops in (a) and rises in (b) left to right. $\gamma_0 = 1.5$, $T = 0.3$. (c) Cycle number at failure N^* , (d) magnitude of stress drop $\Delta \Sigma$, and (e) final degree of shear banding $\langle \dot{\gamma} \rangle_f$ vs waiting time, t_w . Strain amplitude $\gamma_0 = 1.125, 1.250, 1.375, \dots, 2.250$ in curves blue to orange, i.e., top to bottom in (c), bottom to top at right of (d), and with $\gamma_0 = 1.125, 1.25 \dots 1.375$ bottom up and $1.5 \dots 2.25$ top down in (e). Panel (c) only shows cases for which $\Delta \Sigma > 0.1$.

increasing t_w , with $N^* \sim t_w^\alpha$ (panel c). Importantly, therefore, ultra annealed samples $t_w \rightarrow \infty$ are predicted to show an indefinite delay before suddenly failing.

So far, we have characterized the dependence of yielding on the strain amplitude γ_0 and waiting time t_w separately. Its dependence on both parameters is summarized in Fig. 3. Importantly, these color maps suggest the possibility of long delayed (large N^*) and catastrophic (large $\Delta \Sigma$) yielding even at large strain amplitudes, provided the sample age prior to shear is large enough. The strain γ_0 at yielding onset in panel (b) roughly coincides with the end of the linear regime, in which the viscoelastic spectra G' and G'' are constant functions of γ_0 [33].

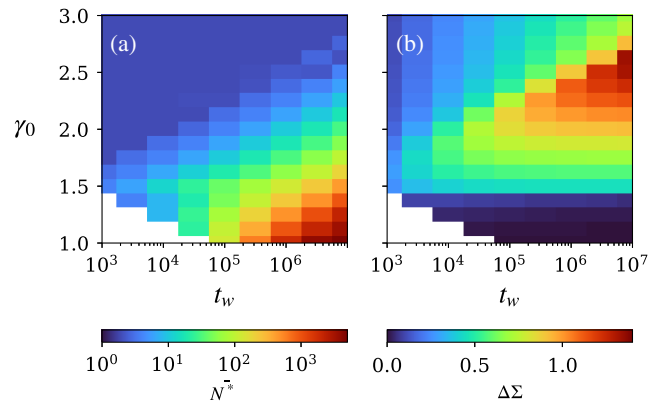


FIG. 3. SGR model. (a) cycle number at failure N^* and (b) stress drop $\Delta \Sigma$ as a function of waiting time t_w and strain amplitude γ_0 . In the white region, no yielding occurs.

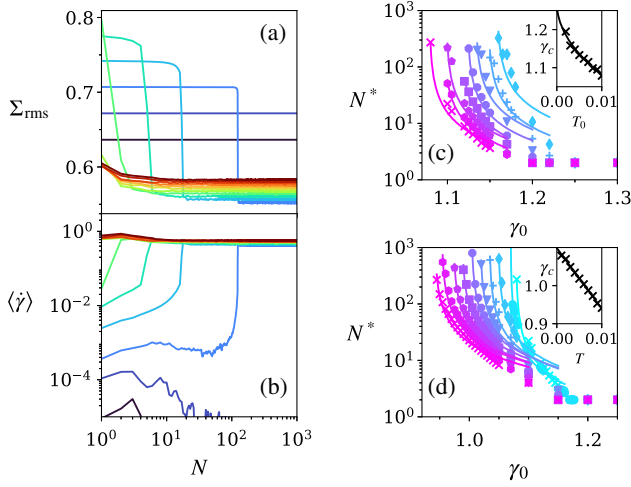


FIG. 4. TEP model. (a) Root mean square stress and (b) mean degree of shear banding over each cycle as a function of cycle number N for strain amplitudes $\gamma_0 = 0.90, 0.95, \dots, 1.50$ in curve sets with drops in (a) and rises in (b) right to left. $T_0 = 0.01$, $T = 0.007$. Cycle number at yielding N^* vs strain amplitude γ_0 for (c) prequench temperatures $T_0 = 0.001, 0.002, \dots, 0.010$ in curves right to left at working temperature $T = 0.001$ and (d) working temperatures $T = 0.001, 0.002, \dots, 0.010$ in curves right to left at prequench temperature $T_0 = 0.01$. Solid lines in (c)+(d) are fits to $N^* = A/(\gamma_0 - \gamma_c)$. Insets show γ_c (symbols) fit (lines) to (c) $\gamma_c = B - C\sqrt{T_0}$ and (d) $\gamma_c = DT - E$.

TEP results.—We now show the same physics to obtain in the TEP model, thereby increasing confidence that it will be generic across many amorphous materials. Figures 4(a), 4(b), and 5(a)–5(d) again show a two-stage yielding process, with strain heterogeneity slowly accumulating and the stress barely declining, before catastrophic failure in which the stress suddenly drops and shear bands form. The number of cycles N^* before failure again increases dramatically with decreasing imposed strain γ_0 , as seen for several prequench temperatures T_0 in Fig. 4(c) and working temperatures T in (d). An interesting difference between TEP and SGR is also apparent. In SGR, recall that N^* increases rapidly with decreasing γ_0 , but with no apparent divergence before the magnitude of yielding becomes negligible [Figs. 1(c)–1(e)]. In TEP, N^* diverges at a nonzero γ_0 for which yielding is still strongly apparent [Figs. 4(c)–4(d)]. Whether this constitutes a fundamental difference between the models or is simply due to our TEP results being for lower T and stronger annealing than are computationally accessible in SGR is unclear.

We now consider the way in which yielding depends in TEP on the degree to which the sample is annealed prior to shear. In Fig. 5(a) and 5(b), a collection of yielding curves for decreasing annealing temperature T_0 in curves left to right demonstrates a dramatically increasing delay before yielding with increasing sample annealing (lower T_0). The number of cycles before yielding is fit to the Boltzmann form $N^* = A \exp(B/T_0)$ in Fig. 5(e). Ultra annealed

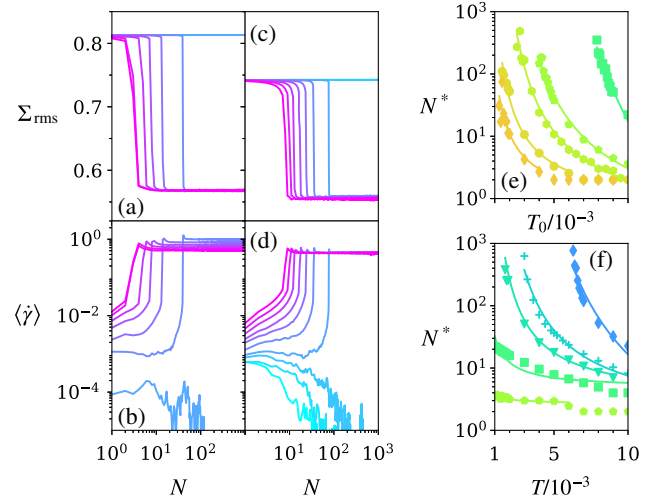


FIG. 5. TEP model. (a) Root mean square stress and (b) mean degree of shear banding over each cycle as a function of cycle number N for prequench temperatures $T_0 = 0.001, 0.002, \dots, 0.010$ in curves with drops in (a),(c) and rises in (b),(d) right to left. $\gamma_0 = 1.15$, $T = 0.001$. (c)+(d) Counterpart curves for working temperatures $T = 0.001, 0.002, \dots, 0.010$ in curves turquoise to magenta. $\gamma_0 = 1.05$, $T_0 = 0.01$. (e) Cycle number at yielding N^* vs prequench temperature T_0 for strain amplitudes $\gamma_0 = 1.10, 1.15, 1.17, 1.20, 1.22$ in curves downward. $T = 0.001$. Solid lines: fits to $N^* = A e^{B/T_0}$. (f) N^* vs working temperature T for $\gamma_0 = 1.00, 1.05, 1.07, 1.10, 1.15$ in curves downward. $T_0 = 0.01$. Solid lines: fits to $N^* = C e^{D/T}$.

samples ($T_0 \rightarrow 0$) are thus predicted in TEP to show indefinitely delayed yielding $N^* \rightarrow \infty$, in close analogy with the corresponding limit $t_w \rightarrow \infty$ in SGR.

We explore finally the dependence of yielding on working temperature T in TEP. A collection of yielding curves left to right in Figs. 5(c) and 5(d) shows a dramatically increasing delay before yielding with decreasing T . The number of cycles before yielding is fit to the Boltzmann form $N^* = A \exp(B/T)$ in Fig. 5(f). Accordingly, then, TEP predicts infinitely delayed yielding in the athermal limit of zero working temperature $T \rightarrow 0$ at fixed strain amplitude γ_0 and prequench temperature T_0 .

Conclusions.—We have shown the yielding of amorphous materials in oscillatory shear to comprise a two-stage process. The first is one of slow fatigue, in which low levels of strain heterogeneity gradually accumulate from cycle to cycle. In the second, the stress drops precipitously and the strain strongly localizes into shear bands, leading to catastrophic material failure. The number of cycles N^* before failure increases dramatically with decreasing imposed strain amplitude and increasing annealing. Finally, N^* diverges in the limit of zero working temperature $T \rightarrow 0$, showing that a small nonzero temperature is indispensable to ultra-delayed yielding.

In future, it would be interesting to consider how the slow fatigue and catastrophic failure studied here (“intercycle

yielding,” over many cycles) relates to the alternating “intracycle” yielding (with shear banding formation) and resolidification (with rehealing to homogeneous shear) that arises in yield stress fluids once a state has been attained that is invariant from cycle to cycle [28,29,32,33]. Another important challenge is to reconcile our divergent N^* in the athermal limit $T \rightarrow 0$ with a finite N^* at $T = 0$ in the mean field study of Ref. [65], which neglects banding. It would also be interesting to model yielding in oscillatory shear stress, as studied experimentally [59–61]. Indeed, any fundamental similarities and differences between delayed yielding in oscillatory shear and other protocols such as creep should also be considered. A fuller exploration of the distinction between ductile and brittle yielding is also warranted [70].

Our predictions are directly testable experimentally. Bulk rheological measurements of the cycle-to-cycle stress can be compared with Figs. 1(a), 1(d), 2(a), 2(d), 3(b), 4(a), 5(a), and 5(c). From these stress measurements, the number of cycles to failure N^* can be extracted and compared with Figs. 1(c), 2(c), 3(a), 4(c), 4(d), 5(e), and 5(f). Ultrasound imaging can be used to measure the velocity field [71], from which the cycle-to-cycle degree of shear banding $\Delta\dot{\gamma}$ can be extracted as prescribed on p2 and compared with our Figs. 1(b), 1(f), 2(b), 2(f), 4(b), 5(b), and 5(d). All these quantities can also be accessed directly in direct particle simulations.

We thank Jack Parley and Peter Sollich for interesting discussions. This project has received funding from the European Research Council (ERC) under the European Union’s Horizon 2020 research and innovation programme (Grant Agreement No. 885146). J. O. C. was supported by the EPSRC funded Centre for Doctoral Training in Soft Matter and Functional Interfaces (SOFI CDT—EP/L015536/1).

[1] A. Nicolas, E. E. Ferrero, K. Martens, and J.-L. Barrat, Deformation and flow of amorphous solids: Insights from elastoplastic models, *Rev. Mod. Phys.* **90**, 045006 (2018).
 [2] D. Bonn, M. M. Denn, L. Berthier, T. Divoux, and S. Manneville, Yield stress materials in soft condensed matter, *Rev. Mod. Phys.* **89**, 035005 (2017).
 [3] L. Berthier and G. Biroli, Theoretical perspective on the glass transition and amorphous materials, *Rev. Mod. Phys.* **83**, 587 (2011).
 [4] S. M. Fielding, Triggers and signatures of shear banding in steady and time-dependent flows, *J. Rheol.* **60**, 821 (2016).
 [5] T. Divoux, D. Tamarii, C. Barentin, and S. Manneville, Transient shear banding in a simple yield stress fluid, *Phys. Rev. Lett.* **104**, 208301 (2010).
 [6] G. P. Shrivastav, P. Chaudhuri, and J. Horbach, Heterogeneous dynamics during yielding of glasses: Effect of aging, *J. Rheol.* **60**, 835 (2016).

[7] V. V. Vasisht and E. Del Gado, Computational study of transient shear banding in soft jammed solids, *Phys. Rev. E* **102**, 012603 (2020).
 [8] V. V. Vasisht, G. Roberts, and E. Del Gado, Emergence and persistence of flow inhomogeneities in the yielding and fluidization of dense soft solids, *Phys. Rev. E* **102**, 010604 (R) (2020).
 [9] T. Divoux, D. Tamarii, C. Barentin, S. Teitel, and S. Manneville, Yielding dynamics of a herschel–bulkley fluid: A critical-like fluidization behaviour, *Soft Matter* **8**, 4151 (2012).
 [10] V. Grenard, T. Divoux, N. Taberlet, and S. Manneville, Timescales in creep and yielding of attractive gels, *Soft Matter* **10**, 1555 (2014).
 [11] R. Benzi, T. Divoux, C. Barentin, S. Manneville, M. Sbragaglia, and F. Toschi, Unified theoretical and experimental view on transient shear banding, *Phys. Rev. Lett.* **123**, 248001 (2019).
 [12] P. Chaudhuri and J. Horbach, Onset of flow in a confined colloidal glass under an imposed shear stress, *Phys. Rev. E* **88**, 040301(R) (2013).
 [13] M. L. Manning, J. S. Langer, and J. M. Carlson, Strain localization in a shear transformation zone model for amorphous solids, *Phys. Rev. E* **76**, 056106 (2007).
 [14] A. R. Hinkle and M. L. Falk, A small-gap effective-temperature model of transient shear band formation during flow, *J. Rheol.* **60**, 873 (2016).
 [15] E. Jagla, Strain localization driven by structural relaxation in sheared amorphous solids, *Phys. Rev. E* **76**, 046119 (2007).
 [16] T. C. Hufnagel, C. A. Schuh, and M. L. Falk, Deformation of metallic glasses: Recent developments in theory, simulations, and experiments, *Acta Mater.* **109**, 375 (2016).
 [17] M. J. Doyle, A. Maranci, E. Orowan, and S. Stork, The fracture of glassy polymers, *Proc. R. Soc. A* **329**, 137 (1972).
 [18] F. Rouyer, S. Cohen-Addad, R. Höhler, P. Sollich, and S. Fielding, The large amplitude oscillatory strain response of aqueous foam: Strain localization and full stress fourier spectrum, *Eur. Phys. J. E* **27**, 309 (2008).
 [19] A. S. Yoshimura and R. K. Prud’homme, Response of an elastic bingham fluid to oscillatory shear, *Rheol. Acta* **26**, 428 (1987).
 [20] V. Viasnoff, S. Jurine, and F. Lequeux, How are colloidal suspensions that age rejuvenated by strain application?, *Faraday Discuss.* **123**, 253 (2003).
 [21] R. H. Ewoldt, P. Winter, J. Maxey, and G. H. McKinley, Large amplitude oscillatory shear of pseudoplastic and elastoviscoplastic materials, *Rheol. Acta* **49**, 191 (2010).
 [22] F. Renou, J. Stellbrink, and G. Petekidis, Yielding processes in a colloidal glass of soft star-like micelles under large amplitude oscillatory shear (LAOS), *J. Rheol.* **54**, 1219 (2010).
 [23] Y. Guo, W. Yu, Y. Xu, and C. Zhou, Correlations between local flow mechanism and macroscopic rheology in concentrated suspensions under oscillatory shear, *Soft Matter* **7**, 2433 (2011).
 [24] K. van der Vaart, Y. Rahmani, R. Zargar, Z. Hu, D. Bonn, and P. Schall, Rheology of concentrated soft and hard-sphere suspensions, *J. Rheol.* **57**, 1195 (2013).

- [25] N. Koumakis, J.F. Brady, and G. Petekidis, Complex oscillatory yielding of model hard-sphere glasses, *Phys. Rev. Lett.* **110**, 178301 (2013).
- [26] A.S. Poulos, J. Stellbrink, and G. Petekidis, Flow of concentrated solutions of starlike micelles under large-amplitude oscillatory shear, *Rheol. Acta* **52**, 785 (2013).
- [27] A. S. Poulos, F. Renou, A. R. Jacob, N. Koumakis, and G. Petekidis, Large amplitude oscillatory shear (LAOS) in model colloidal suspensions and glasses: Frequency dependence, *Rheol. Acta* **54**, 715 (2015).
- [28] S. A. Rogers, B. M. Erwin, D. Vlassopoulos, and M. Cloitre, A sequence of physical processes determined and quantified in laos: Application to a yield stress fluid, *J. Rheol.* **55**, 435 (2011).
- [29] S. A. Rogers and M. P. Lettinga, A sequence of physical processes determined and quantified in large-amplitude oscillatory shear (LAOS): Application to theoretical non-linear models, *J. Rheol.* **56**, 1 (2012).
- [30] P.R. de Souza Mendes and R.L. Thompson, A unified approach to model elasto-viscoplastic thixotropic yield-stress materials and apparent yield-stress fluids, *Rheol. Acta* **52**, 673 (2013).
- [31] B. C. Blackwell and R. H. Ewoldt, A simple thixotropic-viscoelastic constitutive model produces unique signatures in large-amplitude oscillatory shear (LAOS), *J. Non-Newtonian Fluid Mech.* **208–209**, 27 (2014).
- [32] R. Radhakrishnan and S. M. Fielding, Shear banding of soft glassy materials in large amplitude oscillatory shear, *Phys. Rev. Lett.* **117**, 188001 (2016).
- [33] R. Radhakrishnan and S. M. Fielding, Shear banding in large amplitude oscillatory shear (laosstrain and laostress) of soft glassy materials, *J. Rheol.* **62**, 559 (2018).
- [34] J. M. van Doorn, J. E. Verweij, J. Sprakel, and J. van der Gucht, Strand plasticity governs fatigue in colloidal gels, *Phys. Rev. Lett.* **120**, 208005 (2018).
- [35] H. Bhaumik, G. Foffi, and S. Sastry, The role of annealing in determining the yielding behavior of glasses under cyclic shear deformation, *Proc. Natl. Acad. Sci. U.S.A.* **118**, e2100227118 (2021).
- [36] L. Corte, P. M. Chaikin, J. P. Gollub, and D. J. Pine, Random organization in periodically driven systems, *Nat. Phys.* **4**, 420 (2008).
- [37] P. Das, H. Vinutha, and S. Sastry, Unified phase diagram of reversible–irreversible, jamming, and yielding transitions in cyclically sheared soft-sphere packings, *Proc. Natl. Acad. Sci. U.S.A.* **117**, 10203 (2020).
- [38] D. Fiocco, G. Foffi, and S. Sastry, Oscillatory athermal quasistatic deformation of a model glass, *Phys. Rev. E* **88**, 020301(R) (2013).
- [39] T. Kawasaki and L. Berthier, Macroscopic yielding in jammed solids is accompanied by a nonequilibrium first-order transition in particle trajectories, *Phys. Rev. E* **94**, 022615 (2016).
- [40] K. Khirallah, B. Tyukodi, D. Vandembroucq, and C. E. Maloney, Yielding in an integer automaton model for amorphous solids under cyclic shear, *Phys. Rev. Lett.* **126**, 218005 (2021).
- [41] E. D. Knowlton, D. J. Pine, and L. Cipelletti, A microscopic view of the yielding transition in concentrated emulsions, *Soft Matter* **10**, 6931 (2014).
- [42] D. Kumar, S. Patinet, C. Maloney, I. Regev, D. Vandembroucq, and M. Mungan, Mapping out the glassy landscape of a mesoscopic elastoplastic model, *J. Chem. Phys.* **157**, 174504 (2022).
- [43] M. O. Lavrentovich, A. J. Liu, and S. R. Nagel, Period proliferation in periodic states in cyclically sheared jammed solids, *Phys. Rev. E* **96**, 020101(R) (2017).
- [44] P. Leishangthem, A. D. Parmar, and S. Sastry, The yielding transition in amorphous solids under oscillatory shear deformation, *Nat. Commun.* **8**, 1 (2017).
- [45] C. Liu, E. E. Ferrero, E. A. Jagla, K. Martens, A. Rosso, and L. Talon, The fate of shear-oscillated amorphous solids, *J. Chem. Phys.* **156**, 104902 (2022).
- [46] M. Mungan and S. Sastry, Metastability as a mechanism for yielding in amorphous solids under cyclic shear, *Phys. Rev. Lett.* **127**, 248002 (2021).
- [47] K. H. Nagamanasa, S. Gokhale, A. Sood, and R. Ganapathy, Experimental signatures of a nonequilibrium phase transition governing the yielding of a soft glass, *Phys. Rev. E* **89**, 062308 (2014).
- [48] C. Ness and M. E. Cates, Absorbing-state transitions in granular materials close to jamming, *Phys. Rev. Lett.* **124**, 088004 (2020).
- [49] D. J. Pine, J. P. Gollub, J. F. Brady, and A. M. Leshansky, Chaos and threshold for irreversibility in sheared suspensions, *Nature (London)* **438**, 997 (2005).
- [50] N. V. Priezjev, Molecular dynamics simulations of the mechanical annealing process in metallic glasses: Effects of strain amplitude and temperature, *J. Non-Cryst. Solids* **479**, 42 (2018).
- [51] N. V. Priezjev, A delayed yielding transition in mechanically annealed binary glasses at finite temperature, *J. Non-Cryst. Solids* **548**, 120324 (2020).
- [52] I. Regev, T. Lookman, and C. Reichhardt, Onset of irreversibility and chaos in amorphous solids under periodic shear, *Phys. Rev. E* **88**, 062401 (2013).
- [53] S. Sastry, Models for the yielding behavior of amorphous solids, *Phys. Rev. Lett.* **126**, 255501 (2021).
- [54] A. Szulc, O. Gat, and I. Regev, Forced deterministic dynamics on a random energy landscape: Implications for the physics of amorphous solids, *Phys. Rev. E* **101**, 052616 (2020).
- [55] W.-T. Yeh, M. Ozawa, K. Miyazaki, T. Kawasaki, and L. Berthier, Glass stability changes the nature of yielding under oscillatory shear, *Phys. Rev. Lett.* **124**, 225502 (2020).
- [56] A. D. S. Parmar, S. Kumar, and S. Sastry, Strain localization above the yielding point in cyclically deformed glasses, *Phys. Rev. X* **9**, 021018 (2019).
- [57] D. V. Denisov, M. T. Dang, B. Struth, A. Zaccone, G. H. Wegdam, and P. Schall, Sharp symmetry-change marks the mechanical failure transition of glasses, *Sci. Rep.* **5**, 14359 (2015).
- [58] L. Cipelletti, K. Martens, and L. Ramos, Microscopic precursors of failure in soft matter, *Soft Matter* **16**, 82 (2020).
- [59] C. Perge, N. Taberlet, T. Gibaud, and S. Manneville, Time dependence in large amplitude oscillatory shear: A rheo-ultrasonic study of fatigue dynamics in a colloidal gel, *J. Rheol.* **58**, 1331 (2014).

- [60] T. Gibaud, C. Perge, S. B. Lindström, N. Taberlet, and S. Manneville, Multiple yielding processes in a colloidal gel under large amplitude oscillatory stress, *Soft Matter* **12**, 1701 (2016).
- [61] B. Saint-Michel, T. Gibaud, and S. Manneville, Predicting and assessing rupture in protein gels under oscillatory shear, *Soft Matter* **13**, 2643 (2017).
- [62] B. P. Bhowmik, H. Hentchel, and I. Procaccia, Fatigue and collapse of cyclically bent strip of amorphous solid, *Europhys. Lett.* **137**, 46002 (2022).
- [63] F. Kun, M. Costa, R. Costa Filho, J. Andrade, J. Soares, S. Zapperi, and H. J. Herrmann, Fatigue failure of disordered materials, *J. Stat. Mech.* (2007) P02003.
- [64] Z. Sha, S. Qu, Z. Liu, T. Wang, and H. Gao, Cyclic deformation in metallic glasses, *Nano Lett.* **15**, 7010 (2015).
- [65] J. T. Parley, S. Sastry, and P. Sollich, Mean-field theory of yielding under oscillatory shear, *Phys. Rev. Lett.* **128**, 198001 (2022).
- [66] P. Sollich, F. Lequeux, P. Hébraud, and M. E. Cates, Rheology of soft glassy materials, *Phys. Rev. Lett.* **78**, 2020 (1997).
- [67] G. Picard, A. Ajdari, F. Lequeux, and L. Bocquet, Elastic consequences of a single plastic event: A step towards the microscopic modeling of the flow of yield stress fluids, *Eur. Phys. J. E* **15**, 371 (2004).
- [68] C.-Y. D. Lu, P. D. Olmsted, and R. C. Ball, Effects of nonlocal stress on the determination of shear banding flow, *Phys. Rev. Lett.* **84**, 642 (2000).
- [69] If the minimum occurs before the maximum, we argue that the sample does not show yielding for the parameter values in question.
- [70] H. J. Barlow, J. O. Cochran, and S. M. Fielding, Ductile and brittle yielding in thermal and athermal amorphous materials, *Phys. Rev. Lett.* **125**, 168003 (2020).
- [71] S. Manneville, Recent experimental probes of shear banding, *Rheol. Acta* **47**, 301 (2008).